ChemPubSoc Europe

DOI: 10.1002/cmdc.201700589

CHEMMEDCHEM Full Papers

Synthesis, Biological Evaluation and Molecular Modeling Studies of Propargyl-Containing 2,4,6-Trisubstituted Pyrimidine Derivatives as Potential Anti-Parkinson Agents

Bhupinder Kumar, Mohit Kumar, Ashish Ranjan Dwivedi, and Vinod Kumar*[a]

Monoamine oxidase B (MAO-B) inhibitors are potential drug candidates for the treatment of various neurological disorders including Parkinson's disease. A total of 20 new propargyl-containing 2,4,6-trisubstituted pyrimidine derivatives were synthesized and screened for MAO inhibition using Amplex Red assays. All the synthesized compounds were found to be reversible and selective inhibitors of the MAO-B isoform at sub-micromolar concentrations. **MVB3** was the most potent MAO-B inhibitor with an IC_{50} value of 0.38 ± 0.02 μM, whereas **MVB6** ($IC_{50} = 0.51 \pm 0.04$ μM) and **MVB16** ($IC_{50} = 0.48 \pm 0.06$ μM) were the most selective for MAO-B with a selectivity index of more than 100-fold. In cytotoxic studies, these compounds were found to be nontoxic to human neuroblastoma SH-SY5Y cells at concentrations of 25 μM. **MVB6** was found to decrease the intracellular level of reactive oxygen species to 68% at 10 μM concentration, whereas other compounds did not produce significant changes in reactive oxygen species levels. In molecular modeling studies, **MVB3** displayed strong binding affinity for the MAO-B isoform with a dock score of −10.45, in agreement with the observed activity. All the compounds fitted well in the hydrophobic cavity of MAO-B. Thus, propargyl-substituted pyrimidine derivatives can be promising leads in the development of potent, selective and reversible MAO-B inhibitors for the treatment of Parkinson's disease.

Introduction

Parkinson's disease (PD) is a progressive neurological disorder characterized by a myriad of symptoms that gradually affects the patient's daily activities and gradually decreases their quality of life.[1] The pathology of PD is linked with the affected basal ganglia region where the monoamine oxidase B (MAO-B) isoform seems to be mainly responsible for the metabolism of dopamine. MAO-B-mediated metabolism in the glial neurons increases the concentration of the catalytic reaction product H_2O_2 in the brain.[2] This build up promotes apoptotic signaling events in neuronal cells, resulting in decreased levels of dopamine-producing cells.[3] Strategies for the treatment of PD involve increasing the concentration of dopamine in the brain either by the release of dopamine from presynaptic neurons, or by inhibiting its metabolism and reuptake from the synaptic cleft.[4] Inhibitors of the MAO-B isoform have been proposed as potential therapeutic agents for the management or treatment of PD. Selective MAO-B inhibitors (e.g., L-deprenyl, rasagiline) are used alone or in combination with levodopa,[5] a metabolic precursor of dopamine,to maintain dopamine levels for the treatment of PD. However, due to their irreversible mechanism of inhibition, these MAO-B inhibitors are associated with number of side effects that limit their use.[6] However, recent reports on the potential of reversible MAO-B inhibitors in the treatment of PD and their neuroprotective and neurorescue[7] potential is a strong driving force for the discovery of novel potent, selective and reversible MAO-B inhibitors.[8]

Pyrimidine is an important six-membered heterocyclic structure, present in many bioactive compounds.[9] This scaffold was found to be a remarkable building block and around it a variety of novel heterocycles with excellent pharmaceutical profile can be designed.[10] Mathew et al. synthesized a series of novel MAO-A inhibitors based on 1*H*-benzimidazole-bearing pyrimidine-triones (Figure 1a) and screened in vitro for antidepressant activity.[11] Altomare et al. reported condensed pyrimidine derivatives (Figure 1b,c) for their MAO-B inhibitory activity and found potent MAO-B inhibitors with little or no affinity for the MAO-A isoform.[12] The same research group also reported on the synthesis of new pyridazine-, pyrimidine- and 1,2,4-triazine-containing tricyclic derivatives (Figure 1d,e) as potential MAO-B inhibitors.[13] Rasagiline [*N*-propargyl-1(*R*)-aminoindan], is a potent second-generation irreversible MAO-B inhibitor and it has been found that the propargyl group in the molecule

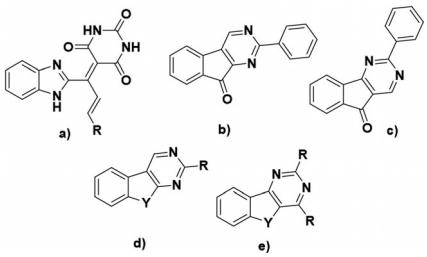

Figure 1. Examples of pyrimidine derivatives that are MAO inhibitors.

[a] *B. Kumar, M. Kumar, A. R. Dwivedi, Dr. V. Kumar*
Department of Pharmaceutical Sciences and Natural Products, Central University of Punjab, Mansa Road, Bathinda, Punjab 151001 (India)
E-mail: vinod.kumar@cup.edu.in

Supporting information and the ORCID identification number(s) for the author(s) of this article can be found under: https://doi.org/10.1002/cmdc.201700589.

plays a crucial role in the MAO-B inhibitory activity.[14] In structure–activity relationship studies, it has been established that the propargyl group promotes neuronal survival via neuroprotective/neurorescue pathways.[15]

In a continuation of our efforts toward the development of selective and potent MAO inhibitors,[2a,8] in the present study, pyrimidine derivatives incorporating a propargyl moiety were designed. The objective of the study was to investigate the effect of propargyl substitution on the MAO inhibition potential of pyrimidine derivatives. Thus, we designed and synthesized a series of 2,4,6-trisubstituted pyrimidine derivatives containing the *O*-propargyl moiety. The synthesized compounds were screened against MAO-A and MAO-B isoforms using an Amplex Red assay. Most of the compounds displayed selectivity for the MAO-B isoform with inhibitory activities in the submicromolar range for MAO-B and low affinities for the MAO-A isoform. Molecular modeling studies were performed and it was found that the synthesized compounds bind with the "entrance" and "substrate" cavities of the MAO-B enzyme. All the compounds were found to be reversible MAO-B inhibitors, and the most potent of them exhibited no cytotoxicity against SH-SY5Y cells even at 25 μM concentration. In addition, reactive oxygen species (ROS) inhibition potential of the representative compounds was also evaluated.

Results and Discussion

Chemistry

All the compounds were synthesized as described in Scheme 1. In brief, *ortho*- and *para*-hydroxy-substituted acetophenones **1** were alkylated using propargyl bromide and potassium carbonate in acetone to obtain 1-[(prop-2-yn-1-yloxy)-phenyl]ethanones **2**. Compounds **2** were reacted with various substituted benzaldehydes through aldol condensation reaction to give (*E*)-3-phenyl-1-[(prop-2-yn-1-yloxy)phenyl]prop-2-en-1-ones **3**. Compounds **3** were further combined with amidines in the presence of sodium carbonate and underwent Michael additions to yield target 2,4,6-trisubstituted pyrimidines **MVB1**–**MVB20** (Scheme 1 and Table 1). The cyclization reaction to form the bridged pyrimidine ring is accompanied by the oxidation process.[16] The structures of the synthesized intermediates were confirmed using IR spectroscopy and ESI-MS and the final products were characterized by IR spectroscopy, ^{1}H and ^{13}C NMR spectroscopy, ESI-MS and HRMS.

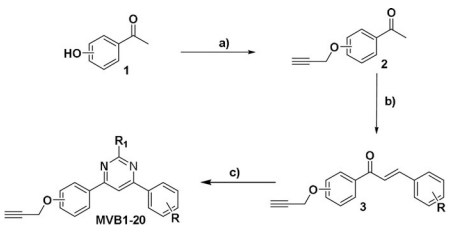

Scheme 1. Synthesis of target compounds **MVB1**–**MVB20**: a) Propargyl bromide (1.2 equiv), K_2CO_3 (2 equiv), acetone, reflux, 12 h; b) substituted benzaldehyde (1 equiv), CH_3OH, 10% aq. NaOH, RT, stirring, 1 h; c) amidine (1.5 equiv), Na_2CO_3 (2.5 equiv), CH_3CN, reflux, 24 h.

Monoamine oxidase inhibition studies

The MAO inhibition potential of the pyrimidine derivatives (**MVB1–MVB20**) was evaluated on recombinant human MAO-A and MAO-B enzymes (purchased from Sigma–Aldrich) using the Amplex Red assay kit.[17] The MAO-A and MAO-B inhibition data for the compounds and standard inhibitors (clorgyline, pargyline) and selectivity indices (SI, the ratio of IC_{50} values of MAO-A/MAO-B) are reported in Table 1. All the synthesized compounds showed low micromolar inhibition activities for the MAO-A isoform and sub-micromolar IC_{50} values against the MAO-B isoform (Table 1). All the compounds in this series were found to be selective for the MAO-B isoform. **MVB3**, with a propargyl group at the *para* position of ring A, a *para*-methyl substituent at ring B and with an amino group on the pyrimidine ring ($R^1 = NH_2$, Table 1) was found to be the most potent MAO-B inhibitor with an IC_{50} value of 0.38 ± 0.02 μM, and showed more than 26-fold selectivity over MAO-A. Replacement of the *para* substituent of ring B with a methoxy group (**MVB1**) or hydrogen (**MVB2**) decreased the activity and selectivity for MAO-B. Similarly, replacement of NH_2 with a phenyl group on the pyrimidine ring (**MVB18**) approximately halves the activity for MAO-B but increases selectivity by more than 50-fold. **MVB5**, with an electron-withdrawing *para*-chloro substituent, showed marginal decreases in MAO-B inhibitory activity and selectivity compared with **MVB3**. The presence of electron-withdrawing groups at the *ortho* (**MVB11**) and *meta* (**MVB15**) positions of ring B produced similar results. A 3,4-dimethoxy substituent on ring B (**MVB6**) significantly increased the selectivity (to more than 100-fold) for the MAO-B isoform. It was observed that in most cases, replacement of the NH_2 on the pyrimidine ring by a phenyl group enhanced selectivity for the MAO-B isoform. **MVB16** was found most selective for the MAO-B isoform with an SI of greater than 104 and an IC_{50} value of 0.48 ± 0.06 μM for MAO-B. Switching the propargyl substitution from the *para* to the *ortho* position of ring A (**MVB8**, **MVB9** and **MVB16**) also increases selectivity for the MAO-B isoform. Interestingly, replacement of NH_2 on the pyrimidine ring by a methyl substituent (**MVB10**) increased MAO-A inhibitory activity and rendered the compound nonselective.

Reversibility studies

As evident from literature reports, a number of side effects are associated with the use of irreversible MAO inhibitors and hence reversibility of MAO inhibition is frequently considered in the design and development of new candidates. To determine the reversibility of synthesized compounds, experiments were performed using reported protocols.[18] An effective dilution method was applied and pargyline (an irreversible drug) was used as a standard. The test compounds (concentrations of $10 \times IC_{50}$ and $100 \times IC_{50}$) were pre-incubated for 30 min with MAO-B and enzymatic activity was determined using the method used for the MAO inhibition studies. After the pre-in-

Table 1. MAO inhibition studies on the synthesized compounds. All compounds were evaluated against MAO-A and MAO-B isoforms, and the selectivity of the ligands was determined.

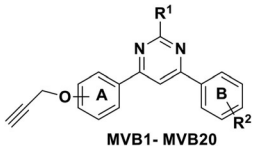

MVB1- MVB20

Compound	R^1	R^2	Propargyl group position	IC_{50} [μM][a]		SI IC_{50} MAO-A/IC_{50} MAO-B	MAO selectivity	Reversibility
				MAO-A	MAO-B			
MVB1	NH_2	4-OCH_3	C4	8.83 ± 0.13	0.53 ± 0.06	17	MAO-B	reversible
MVB2	NH_2	H	C4	9.91 ± 0.21	0.59 ± 0.19	17	MAO-B	reversible
MVB3	NH_2	4-CH_3	C4	9.97 ± 0.11	0.38 ± 0.02	26	MAO-B	reversible
MVB4	C_6H_5	H	C4	9.83 ± 0.07	0.69 ± 0.16	14	MAO-B	reversible
MVB5	NH_2	4-Cl	C4	9.15 ± 0.09	0.50 ± 0.17	18	MAO-B	reversible
MVB6	NH_2	3,4-di-OCH_3	C4	> 50[b]	0.51 ± 0.04	> 100	MAO-B	reversible
MVB7	C_6H_5	3,4-di-OCH_3	C4	25.01 ± 0.15	0.60 ± 0.02	42	MAO-B	reversible
MVB8	NH_2	4-Cl	C2	20.32 ± 0.11	0.70 ± 0.08	29	MAO-B	reversible
MVB9	C_6H_5	4-Br	C2	19.63 ± 0.21	0.56 ± 0.06	35	MAO-B	reversible
MVB10	CH_3	4-OCH_3	C4	0.90 ± 0.04	0.52 ± 0.02	2	MAO-B	reversible
MVB11	NH_2	2-F	C4	10.94 ± 0.24	0.60 ± 0.03	18	MAO-B	reversible
MVB12	NH_2	2-OCH_3	C4	21.86 ± 0.31	0.63 ± 0.11	35	MAO-B	reversible
MVB13	C_6H_5	2-F	C4	> 50[b]	0.87 ± 0.16	57	MAO-B	reversible
MVB14	C_6H_5	2-OCH_3	C4	> 50[b]	0.55 ± 0.05	91	MAO-B	reversible
MVB15	NH_2	3-Cl	C4	16.54 ± 0.16	0.69 ± 0.23	24	MAO-B	reversible
MVB16	C_6H_5	4-Cl	C2	> 50[b]	0.48 ± 0.06	104	MAO-B	reversible
MVB17	C_6H_5	4-Cl	C4	23.77 ± 0.28	0.44 ± 0.14	55	MAO-B	reversible
MVB18	-C_6H_5	4-CH_3	C4	> 50[b]	0.66 ± 0.18	76	MAO-B	reversible
MVB19	C_6H_5	3-Cl	C4	> 50[b]	0.56 ± 0.27	89	MAO-B	reversible
MVB20	C_6H_5	4-OCH_3	C4	4.61 ± 0.15	0.55 ± 0.08	8	MAO-B	reversible
Clorgyline		–		4.39 ± 1.02 nM	–	–	MAO-A	irreversible
Pargyline		–		–	0.15 ± 0.02	–	MAO-B	irreversible

[a] Values are the mean ± SEM ($n = 3$). [b] Showed < 50% inhibition at 50 μM, and compound precipitated at higher concentrations.

cubation period, the test compound was diluted to 0.1 × IC_{50} and 1 × IC_{50} (final concentrations) by adding 200 μM Amplex Red reagent, 1 U mL^{-1} horseradish peroxidase and 1 mM *p*-tyramine, and the solution was further incubated for 30 min. Thereafter the MAO-B enzyme activity was determined again.

All the compounds were found to be reversible inhibitors of the MAO-B isoform. Notably, most of the published MAO inhibitors containing a propargyl group bind the enzyme in an irreversible manner. The irreversibility of these drugs is attributed to the strong covalent interactions of the propargyl group (attached through C and N atoms) at the receptor site. However, the current series of compounds with the propargyl substituent was found to be reversible, which might be due to the attachment of the propargyl group to an oxygen atom (O-alkylated). Mertens et al. also reported a series of *O*-alkynyl coumarinyl compounds, including *O*-propargyl-substituted derivatives, as reversible inhibitors of MAO-A and MAO-B isoforms.[19] The results of reversibility studies of some of the most potent (**MVB3**) and highly selective MAO-B inhibitors (**MVB6**, **MVB14** and **MVB16**) are shown in Table 2. **MVB6** showed 85% recovery in the MAO-B activity on 100-fold dilution of the substrate. Similarly, **MVB16** showed recovery in MAO-B activity up to 82% in the reversibility studies. **MVB3**, the most potent MAO-B inhibitor in the series, showed recovery in the enzyme activity of up to 71%.

Table 2. Reversibility studies of representative synthesized compounds against the MAO-B isoform.

Compound	MAO-B activity [%][a]			
	10 × IC_{50}	100 × IC_{50}	0.1 × IC_{50}	1 × IC_{50}
MVB3	8 ± 0.49	5 ± 0.21	71 ± 2.53	40 ± 1.33
MVB6	11 ± 0.63	4 ± 0.14	85 ± 1.76	46 ± 0.94
MVB14	9 ± 0.82	2 ± 0.18	73 ± 1.89	29 ± 1.21
MVB16	13 ± 1.65	3 ± 0.05	82 ± 2.63	30 ± 0.75
Pargyline	7 ± 0.31	–	8 ± 0.11	–

[a] Values are the mean ± SEM relative to control (100%), $n = 3$; concentrations of test compound used were 10 × IC_{50} and 100 × IC_{50} and diluted to 0.1 × IC_{50} and 1 × IC_{50}.

Cytotoxicity studies

The cytotoxic effects of representative compounds **MVB3**, **MVB6**, **MVB14** and **MVB16** were evaluated in human neuroblastoma SH-SY5Y cells, because of their similarity to dopaminergic neurons. The compounds were incubated at 25 μM concentration with cells and their effects were analyzed after 24 and 48 h. The percentage of viable cells was measured using the MTT assay. As depicted in Table 3, the compounds were found to be nontoxic against the tested cells. **MVB6** displayed cell viability of 114% relative to the control cells after 24 h and 101% after 48 h of treatment. The lowest cell viability of 85%

Table 3. Cytotoxicity studies of representative compounds against SH-SY5Y cells.

Compound	Cell viability [%][a]	
	After 24 h	After 48 h
MVB3	97 ± 3	100 ± 2
MVB6	114 ± 4	101 ± 3
MVB14	88 ± 2	86 ± 4
MVB16	93 ± 3	85 ± 5

[a] Values are the mean ± SEM relative to control (100%), $n = 3$; the concentration of test compounds used was 25 μM. All compounds were found to be nontoxic.

Table 4. Intracellular ROS levels in SH-SY5Y cells after treatment with the most active and selective compounds.

Compound	ROS level [%][a]	
	1 μM	10 μM
MVB3	97 ± 4	96 ± 2
MVB6	80 ± 3	67 ± 2
MVB14	81 ± 4	72 ± 3
MVB16	144 ± 6	80 ± 3

[a] Values are the mean ± SEM relative to control (100%), $n = 3$.

was observed after a 48 h treatment with **MVB16**, and all other compounds resulted in more than 85% of cell viability. Thus, considering the IC_{50} value obtained for MAO-B inhibition, the current series of compounds were found to be nontoxic to cells.

Intracellular reactive oxygen species determination

MAO-mediated metabolism of monoamines generates H_2O_2 as a by-product.[20] Iron-mediated breakdown of H_2O_2 into free radicals (•OH) is responsible for the oxidative stress and subsequent neural cell damage. Increased levels of ROS can cause oxidative damage to cell membranes and DNA strand breakage. Thus, prevention of ROS generation along with MAO inhibition is an important strategy to prevent neurotoxicity in neurodegenerative diseases.

Intracellular ROS levels of SH-SY5Y cells were determined using the nonfluorescent compound 2′,7′-dichlorodihydrofluorescein diacetate (H_2DCF-DA). This compound is cell permeable and is oxidized by ROS to a fluorescent compound, 2′,7′-dichlorofluorescein. Treatment of cells with **MVB6** (10 μM) decreased the intracellular level to 68%, whereas **MVB16** (1 μM) increased the intracellular level to 144%, but decreased the ROS level at the higher concentration (10 μM). The other tested compounds did not significantly effect the intracellular ROS levels (Table 4).

Molecular docking studies

To rationalize the orientations and interactions of ligands at the receptor site, molecular modeling studies were performed. The binding affinities of the most potent and selective compounds were calculated in MAO-B receptor models through docking simulations. **MVB3** and **MVB16** were docked at hMAO-B (PDB ID: 2BYB).[21] The volume of the MAO-B cavity is approximately 700 Å^3 and it was found to be bipartite, containing two separate spaces: the substrate cavity (≈400 Å^3) and the entrance cavity (≈300 Å^3).[22] The position of the flavin adenine dinucleotide (FAD) cofactor with respect to the overall structure is highly conserved and the substrate-binding sites consist of elongated cavities.[23] Separating the entrance cavity from the similarly hydrophobic substrate cavity (volume = 400 Å^3) is the side chain of Ile199, which serves as a "gate" between the two cavities. The two cavities are hydrophobic, involving two nearly parallel tyrosyl residues (398 and 435), which form an "aromatic cage".[24] The hydrophilic section is near the flavin and is essential for recognition and directionality of the amine functionality of the substrate. This hydrophilic region is located between Tyr398 and Tyr435, which together with the flavin, form an aromatic cage for amine recognition. The docking studies were performed using Maestro 11.1 (Schrödinger LLC) and first validated by accurately re-docking the co-crystallized ligands into the MAO-B model. On docking with a co-crystallized ligand, it was found that Tyr60, Phe103, Tyr326, Tyr398 and Tyr435 are important amino acids that line the hydrophobic pocket of the MAO-B active site. Ile199 and Tyr326 are important amino acids that separate the entrance cavity from the ligand binding cavity. Amongst the ligands, **MVB3**, with a docking score of −10.45, showed the highest binding affinity for the MAO-B isoform. **MVB3** was found to fit in the hydrophobic cavity of MAO-B aligned with residues Tyr60, Tyr188, Tyr326, Tyr398, Phe99, Phe103, Phe343 and FAD (Figure 2A and B). The propargyl group in **MVB3** was extended toward the entrance cavity, leaving the gate residue Ile199 in the open-gate conformation. **MVB3** was involved in π–π interactions with Tyr326 and Tyr435, which helped stabilize the binding of the ligand at the MAO-B active site. A similar orientation pattern was observed with **MVB16**, of which the propargyl group was oriented toward the entrance cavity (Figure 2C and D). **MVB16** also engaged in a π–π interaction between its *p*-chloro-substituted phenyl ring and Tyr326.

Conclusions

MAO-B inhibitors were investigated as therapeutic agents for the treatment or management of PD. A series of new 2,4,6-trisubstituted pyrimidine derivatives incorporating an *O*-propargyl moiety were synthesized and screened as MAO inhibitors using an Amplex Red assay. All the compounds were found to be selective inhibitors of the MAO-B isoform at sub-micromolar concentrations. A structure–activity relationship profile was developed with the number of electron-donating and electron-withdrawing substituents attached to the aromatic rings. **MVB3** was found to be the most potent MAO-B inhibitor with an IC_{50} value of 0.38 ± 0.02 μM, whereas **MVB16** with an IC_{50} value of 0.48 ± 0.06 μM and **MVB6** with IC_{50} value of 0.51 ± 0.04 μM were the most selective MAO-B inhibitors with an SI of greater than 100. In the reversibility studies, all the tested compounds were found to be reversible inhibitors of the MAO-B

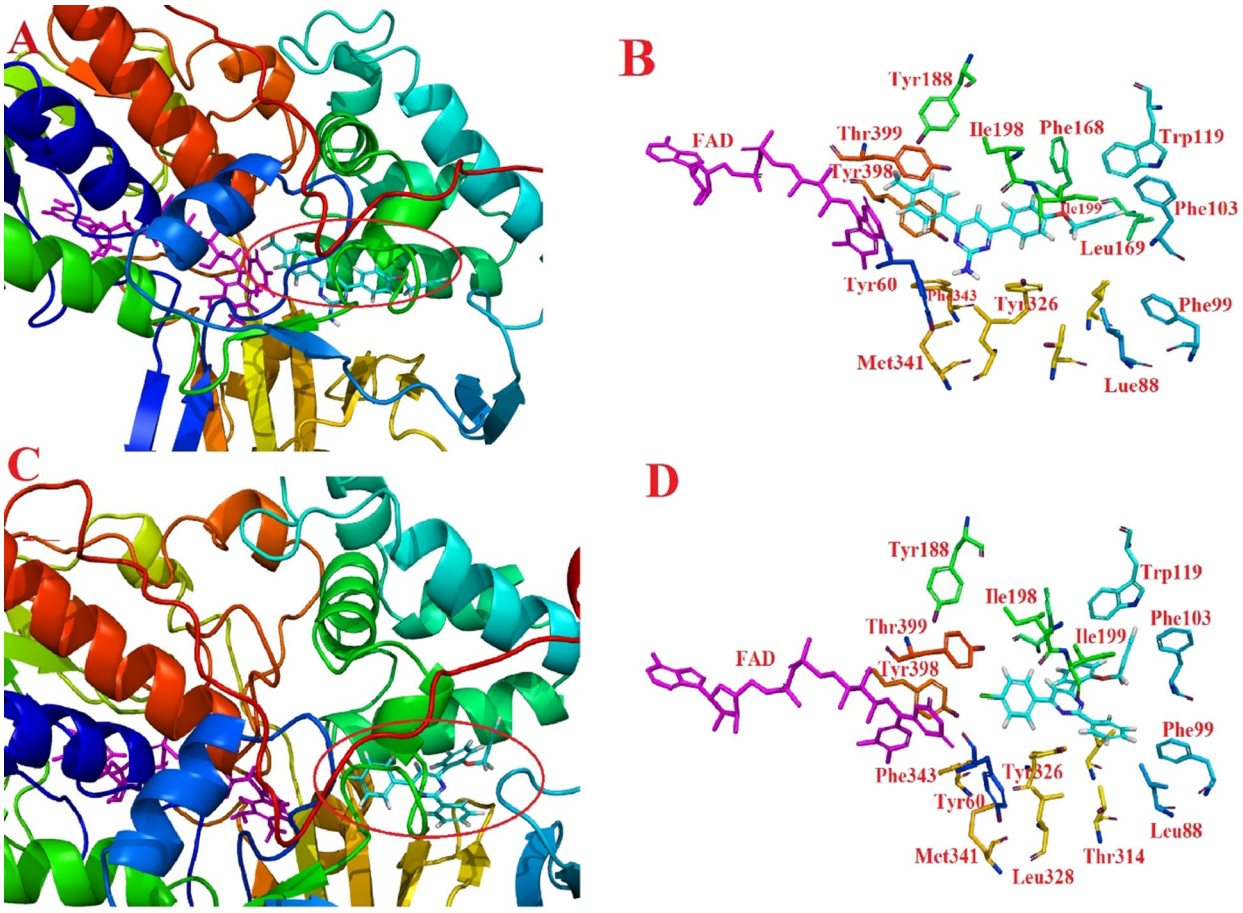

Figure 2. A) Orientation of **MVB3** (cyan) in the MAO-B cavity with the cofactor FAD (purple). B) Binding interactions of **MVB3** (cyan) with the active-site residues of MAO-B. C) Orientation of **MVB16** (cyan) in the MAO-B cavity with the cofactor FAD (purple). D) Binding interactions of **MVB16** (cyan) with the active-site residues of MAO-B.

isoform. The most active and selective compounds were tested for cytotoxicity and found to be safe against human neuroblastoma SH-SY5Y cells at 25 μM. From molecular docking studies, it was found that compounds fit well in the active site of the MAO-B isoform near the FAD cofactor. Thus, the active compounds such as **MVB3**, **MVB14** and **MVB16** obtained in this series can be promising leads for the development of pyrimidine-based potent MAO-B inhibitors for the treatment of Parkinson's disease.[25]

Experimental Section

Materials and Methods

All chemicals and reagents used for the synthesis were purchased from suppliers such as Sigma–Aldrich, Loba-Chemie Pvt. Ltd., and S.D. Fine Chemicals and used without further purification. Thin layer chromatography (TLC) was performed on glass plates coated with silica gel G as the adsorbent; spots were visualized under UV light and iodine chamber. A gradient solvent system of ethyl acetate/petroleum ether (from 1:10 to 1:3), was used for the chromatographic purification of the compounds. Melting points of the synthesized compounds were recorded with Stuart SMP-30 melting point apparatus and are uncorrected. Mass spectra were recorded on a GC–MS (ESI) instrument at the Central Instruments Laboratory, Central University of Punjab, Bathinda (India). ^{1}H and ^{13}C NMR spectra were recorded in $CDCl_3$ containing tetramethylsilane as an internal standard on a Bruker Avance II spectrometer at 400 MHz (100 MHz for ^{13}C) at Panjab University, Chandigarh (India) and a Jeol 400 MHz spectrometer at IIT Ropar, Rupnagar (India). The chemical shifts are reported in parts per million (δ) downfield from the signal of tetramethylsilane ($\delta = 0$ ppm) added to the deuterated solvent. Spin multiplicities are reported as s (singlet), b (broad), d (doublet), dd (doublet of doublets), t (triplet), q (quartet) or m (multiplet). The Invitrogen Amplex Red MAO kit was purchased from Thermo Fisher Scientific. Recombinant hMAO-A and hMAO-B enzymes were purchased from Sigma–Aldrich. A Shimadzu spectrophotometer (UV-1800) was used for UV/Vis absorption studies. Fluorescence was measured using a BioTek microplate reader. Molecular modeling studies were carried out using Maestro 11.1 (Schrödinger LLC) and ChemBioDraw Ultra 12.

Chemistry

General procedure for the preparation of 1-[(prop-2-yn-1-yloxy)-phenyl]ethan-1-ones (2): Propargyl bromide (1.2 equiv) was added dropwise to a mixture of the hydroxyacetophenone (**1**, 2 g) and potassium carbonate (2.4 equiv) in acetone (30 mL). The reaction mixture was heated at reflux for 12 h at 60 °C. The progress of re-

action was monitored by TLC. After completion of the reaction, excess solvent was evaporated from the mixture under vacuum using a rotary evaporator. Water was added to the crude mixture, which was extracted with ethyl acetate (10 mL×3). The combined organic layers were washed with brine, dried over anhydrous Na_2SO_4 and concentrated under vacuum using a rotary evaporator to obtain the crude product **2**.

General procedure for the preparation of (*E*)-3-phenyl-1-[(prop-2-yn-1-yloxy)phenyl]prop-2-en-1-one derivatives (3): An aqueous solution of sodium hydroxide (20%) was added slowly to a mixture of **2** (1 equiv) and substituted aldehyde (1 equiv) in methanol (20 mL) with constant stirring. The reaction mixture was stirred for 1 h at room temperature. The completion of reaction was monitored by TLC. After completion of reaction, excess solvent was evaporated from the mixture under vacuum using a rotary evaporator. Ice-cold water was poured into the reaction mixture and the resulting precipitate was filtered and dried to obtain intermediate **3**.

General procedure for the preparation of MVB1–MVB20: A mixture of **3** (500 mg), amidine (1.2 equiv) and anhydrous sodium carbonate (2.4 equiv) in acetonitrile (5 mL) was heated at reflux at 85 °C for 24 h. The progress of reaction was monitored by TLC. After completion of the reaction, excess solvent was evaporated from the mixture under vacuum using a rotary evaporator. Water added to the residue and the mixture was extracted with ethyl acetate (10 mL×3). The combined organic layers were washed with water, brine, dried over anhydrous Na_2SO_4, and concentrated under vacuum using a rotary evaporator. The crude product was purified by column chromatography (EtOAc/pet ether). The purified compounds were characterized by melting point measurement, mass spectrometry and NMR spectroscopy.

4-(4-Methoxyphenyl)-6-[4-(prop-2-yn-1-yloxy)phenyl]pyrimidin-2-amine (MVB-1): Cream solid. Yield: 62%; m.p. 118–120 °C; ^{1}H NMR ($CDCl_3$, 400 MHz): δ = 8.04–8.01 (m, 4H), 7.35 (s, 1H), 7.08–6.98 (m, 4H), 5.22 (s, 2H), 4.75 (s, 2H), 3.86 (s, 3H), 2.55 ppm (s, 1H); ^{13}C NMR ($CDCl_3$, 100 MHz): δ = 165.55, 165.33, 163.59, 161.66, 159.45, 131.24, 130.27, 128.66, 115.06, 114.15, 102.92, 77.45, 75.97, 55.92, 55.50 ppm; HRMS: *m/z*: calcd for $C_{20}H_{17}N_3O_2$: 332.1399 $[M+H]^+$; found: 332.1380.

4-Phenyl-6-[4-(prop-2-yn-1-yloxy)phenyl]pyrimidin-2-amine (MVB-2): Orange solid. Yield: 72%; m.p. 117–119 °C; ^{1}H NMR ($CDCl_3$, 400 MHz): δ = 8.06–8.02 (m, 4H), 7.50–7.46 (m, 3H), 7.40 (s, 1H), 7.09–7.06 (m, 2H), 5.28 (s, 2H), 4.75 (s, 2H), 2.55 ppm (s, 1H); ^{13}C NMR ($CDCl_3$, 100 MHz): δ = 166.16, 165.59, 163.66, 159.55, 137.94, 131.08, 130.48, 128.70, 127.18 115.10, 103.72, 78.25, 76.00, 55.93 ppm; HRMS: *m/z*: calcd for $C_{19}H_{15}N_3O$: 302.1293 $[M+H]^+$; found: 302.1264.

4-[4-(Prop-2-yn-1-yloxy)phenyl]-6-(*p*-tolyl)pyrimidin-2-amine (MVB-3): Orange solid. Yield: 71%; m.p. 103–105 °C; ^{1}H NMR ($CDCl_3$, 400 MHz): δ = 8.05–8.02 (m, 2H), 7.95–7.93 (m, 2H), 7.38 (s, 1H), 7.29 (s, 2H), 7.08–7.05 (m, 2H), 5.25 (s, 2H), 4.75 (s, 2H), 2.55 (s, 1H), 2.42 ppm (s, 3H); ^{13}C NMR ($CDCl_3$, 100 MHz): δ = 166.07, 165.47, 163.66, 159.51, 140.80, 135.08, 131.21, 129.60, 128.70, 127.11 115.09, 103.43, 77.47, 76.00, 55.94 ppm; HRMS: *m/z*: calcd for $C_{20}H_{17}N_3O$: 316.1450 $[M+H]^+$; found: 316.1434

2,4-Diphenyl-6-[4-(prop-2-yn-1-yloxy)phenyl]pyrimidine (MVB-4): Yellow solid. Yield: 70%; m.p. 118–120 °C; ^{1}H NMR ($CDCl_3$, 400 MHz): δ = 8.73–8.71 (m, 2H), 8.29–8.27 (m, 4H), 7.94 (s, 1H), 7.56–7.52 (m, 6H), 7.15–7.13 (m, 2H), 4.78 (s, 2H), 2.58 ppm (s, 1H) 2.42 (s, 3H); ^{13}C NMR ($CDCl_3$, 100 MHz): δ = 164.57, 164.41, 164.09, 159.80, 138.30, 137.69, 130.70, 130.58, 128.80, 128.47, 128.44, 127.27, 115.21, 109.53, 78.20, 75.94, 55.93 ppm; HRMS: *m/z*: calcd for $C_{25}H_{18}N_2O$: 363.1497 $[M+H]^+$; found: 363.1476.

4-(4-Chlorophenyl)-6-[4-(prop-2-yn-1-yloxy)phenyl]pyrimidin-2-amine (MVB-5): Yellow solid. Yield: 78%; m.p. 148–150 °C; ^{1}H NMR ($CDCl_3$, 400 MHz): δ = 8.01–7.94 (m, 4H), 7.44–7.42 (m, 2H), 7.33 (s, 1H), 7.07–7.04 (2H, m), 5.24 (2H, s), 4.74 (2H, s), 2.54 ppm (1H, s); ^{13}C NMR ($CDCl_3$, 100 MHz): δ = 165.87, 164.86, 163.55, 159.66, 136.65, 130.80, 129.07, 128.72, 128.48, 115.14, 103.47, 78.00, 76.03, 55.93 ppm; HRMS: *m/z*: calcd for $C_{19}H_{15}ClN_3O$: 336.0904 $[M+H]^+$; found: 336.0902.

4-(3,4-Dimethoxyphenyl)-6-[4-(prop-2-yn-1-yloxy)phenyl]pyrimidin-2-amine (MVB-6): Orange solid. Yield: 76%; m.p. 158–160 °C; ^{1}H NMR ($CDCl_3$, 400 MHz): δ = 7.94–7.91 (m, 2H, m), 7.58 (d, *J* = 2 Hz, 1H), 7.50 (dd, *J* = 8, 4 Hz, 1H), 7.26 (s, 1H), 6.98–6.95 (m, 2H), 6.84 (d, *J* = 8 Hz, 1H) 5.13 (s, 2H), 4.65 (s, 2H), 3.86 (d, *J* = 4 Hz, 6H), 2.45 ppm (s, 1H); ^{13}C NMR ($CDCl_3$, 100 MHz): δ = 165.54, 165.35, 163.56, 159.48, 151.17, 149.22, 131.19, 130.56, 128.66, 120.14, 115.07, 110.90, 109.91, 103.03, 78.26, 75.98, 56.09, 55.92 ppm; HRMS: *m/z*: calcd for $C_{21}H_{19}N_3O_3$: 362.1505 $[M+H]^+$; found: 362.1485.

4-(3,4-Dimethoxyphenyl)-2-phenyl-6-[4-(prop-2-yn-1-yloxy)phenyl]pyrimidine (MVB-7): Yellow solid. Yield: 74%; m.p. 140–142 °C; ^{1}H NMR ($CDCl_3$, 400 MHz): δ = 8.70–8.68 (m, 2H), 8.28–8.26 (m, 2H), 7.92 (d, *J* = 4 Hz, 1H), 7.87 (s, 1H), 7.79 (dd, *J* = 8, 4 Hz, 1H), 7.54–7.51 (m, 3H) 7.15–7.13 (m, 2H), 7.00 (d, *J* = 4 Hz, 1H), 4.78 (s, 2H), 4.06 (s, 3H), 3.97 (s, 3H) 2.57 ppm (s, 1H); ^{13}C NMR ($CDCl_3$, 100 MHz): δ = 164.26, 164.11, 163.86, 159.75, 151.48, 149.39, 138.39, 131.01, 130.63, 130.44, 128.84, 128.53, 120.36, 115.21, 111.05, 110.10, 108.91, 78.26, 76.05, 56.18, 56.13, 55.96 ppm; HRMS: *m/z*: calcd for $C_{27}H_{22}N_2O_3$: 423.1709 $[M+H]^+$; found: 423.1696

4-(4-Chlorophenyl)-6-[2-(prop-2-yn-1-yloxy)phenyl]pyrimidin-2-amine (MVB-8): Orange solid. Yield: 75%; m.p. 160–162 °C; ^{1}H NMR ($CDCl_3$, 400 MHz): δ = 8.00–7.98 (m, 2H), 7.87 (dd, *J* = 8, 4 Hz, 1H), 7.64 (s, 1H), 7.44–7.39 (m, 3H), 7.14–7.09 (m, 2H) 5.24 (s, 2H), 4.75 (s, 2H), 2.53 ppm (s, 1H); ^{13}C NMR ($CDCl_3$, 100 MHz): δ = 164.78, 163.95, 163.50, 155.74, 136.44, 131.19, 130.94, 128.98, 128.62, 128.92, 122.24, 113.44, 108.98, 78.44, 75.99, 56.67 ppm; HRMS: *m/z*: calcd for $C_{19}H_{14}ClN_3O$: 336.0904 $[M+H]^+$; found: 336.0879.

4-(4-Bromophenyl)-2-phenyl-6-[2-(prop-2-yn-1-yloxy)phenyl]pyrimidine (MVB-9): Yellow solid. Yield: 69%; m.p. 131–133 °C; ^{1}H NMR ($CDCl_3$, 400 MHz): δ = 8.67–8.65 (m, 2H), 8.33 (s, 1H), 8.27 (dd, *J* = 8, 4 Hz, 1H), 8.17–8.15 (m, 2H), 7.67–7.65 (m, 2H), 7.52–7.48 (m, 4H), 7.24–7.19 (m, 1H), 7.13 (d, *J* = 8 Hz, 1H), 4.81 (s, 2H), 2.57 ppm (s, 1H); ^{13}C NMR ($CDCl_3$, 100 MHz): δ = 164.41, 163.28, 162.69, 156.29, 138.28, 136.84, 132.08, 131.61, 130.61, 129.01, 128.50, 128.43, 127.59, 125.22, 122.38, 115.23, 113.40, 78.38, 76.05, 56.80 ppm; HRMS: *m/z*: calcd for $C_{25}H_{17}BrN_2O$: 441.0603$[M+H]^+$; found: 441.0590.

4-(4-Methoxyphenyl)-2-methyl-6-[4-(prop-2-yn-1-yloxy)phenyl]-pyrimidine (MVB-10): Yellow solid. Yield: 78%; m.p. 132–134 °C; ^{1}H NMR ($CDCl_3$, 400 MHz): δ = 8.11–8.08 (m, 4H), 7.76 (s, 1H), 7.10–7.08 (m, 2H), 7.02–7.00 (m, 2H), 4.76 (s, 2H), 3.87 (s, 3H), 2.81 (s, 3H), 2.55 ppm (s, 1H); ^{13}C NMR ($CDCl_3$, 100 MHz): δ = 168.36, 164.20, 163.99, 161.84, 159.63, 131.09, 130.68, 128.76, 115.27, 114.34, 108.47, 78.25, 75.94, 55.95, 55.49, 26.56 ppm; HRMS: *m/z*: calcd for $C_{21}H_{18}N_2O_2$: 331.1447 $[M+H]^+$; found: 331.1422.

4-(2-Fluorophenyl)-6-[4-(prop-2-yn-1-yloxy)phenyl]pyrimidin-2-amine (MVB-11): Yellow solid. Yield: 68%; m.p. 108–110 °C; ^{1}H NMR ($CDCl_3$, 400 MHz): δ = 8.03–7.98 (m, 3H), 7.48 (d, *J* = 8 Hz, 1H),

7.44–7.39 (m, 1H), 7.27–7.24 (m, 1H), 7.18–7.14 (m, 1H), 7.05 (d, $J=8$ Hz, 2H), 5.22 (s, 2H), 4.74 (s, 2H), 2.54 ppm (s, 1H); ^{13}C NMR ($CDCl_3$, 100 MHz): $\delta=165.44$, 163.51, 162.00, 159.61, 131.73, 130.69, 128.81, 124.64, 116.58, 116.36, 115.09, 107.72, 107.62, 78.23, 75.99, 55.91 ppm; HRMS: *m/z*: calcd for $C_{19}H_{14}FN_3O$: 320.1199 $[M+H]^+$; found: 320.1184.

4-(2-Methoxyphenyl)-6-[4-(prop-2-yn-1-yloxy)phenyl]pyrimidin-2-amine (MVB-12): Yellow solid. Yield: 65%; m.p. 104–106 °C; ^{1}H NMR ($CDCl_3$, 400 MHz): $\delta=8.01$–7.98 (m, 2H), 7.79 (dd, $J=8$, 4 Hz, 1H), 7.53 (s, 1H), 7.42–7.38 (m, 1H), 7.08–7.03 (m, 3H), 7.00 (d, $J=8$ Hz, 1H), 5.19 (s, 2H), 4.74 (s, 2H), 3.87 (s, 3H), 2.53 ppm (s, 1H); ^{13}C NMR ($CDCl_3$, 100 MHz): $\delta=164.92$, 164.54, 163.43, 159.40, 157.59, 131.34, 131.10, 130.70, 128.77, 127.51, 121.09, 115.02, 111.58, 108.52, 77.45, 75.94, 55.90 ppm; HRMS: *m/z*: calcd for $C_{20}H_{17}N_3O_2$: 332.1399 $[M+H]^+$; found: 332.1363.

4-(2-Fluorophenyl)-2-phenyl-6-[4-(prop-2-yn-1-yloxy)phenyl]pyrimidine (MVB-13): Yellow solid. Yield: 62%; m.p. 102–104 °C; ^{1}H NMR ($CDCl_3$, 400 MHz): $\delta=8.69$–8.66 (m, 2H), 8.40–8.36 (m, 1H), 8.27–8.25 (m, 2H), 8.07 (d, $J=8$ Hz, 1H) 7.53–7.48 (m, 4H), 7.36–7.32 (m, 1H), 7.24–7.21 (m, 1H), 7.14–7.11 (m, 2H), 4.77 (s, 2H), 2.56 ppm (s, 1H); ^{13}C NMR ($CDCl_3$, 100 MHz): $\delta=164.42$, 164.04, 162.85, 160.74, 160.34, 159.91, 138.25, 132.07, 131.17, 130.58, 128.97, 128.46, 124.76, 116.61, 116.38, 115.27, 113.81, 78.26, 75.99, 55.97 ppm; HRMS: *m/z*: calcd for $C_{25}H_{17}FN_2O$: 381.1403 $[M+H]^+$; found: 381.1391.

4-(2-Methoxyphenyl)-2-phenyl-6-[4-(prop-2-yn-1-yloxy)phenyl]-pyrimidine (MVB-14): Cream solid. Yield: 64%; m.p. 96–98 °C; ^{1}H NMR ($CDCl_3$, 400 MHz): $\delta=8.68$–8.66 (m, 2H), 8.31–8.21 (m, 4H), 7.51–7.46 (m, 4H), 7.15–7.11 (m, 3H), 7.05 (d, $J=8$ Hz, 1H), 4.77 (s, 2H), 3.94 (s, 3H), 2.54 ppm (s, 1H); ^{13}C NMR ($CDCl_3$, 100 MHz): $\delta=$ 164.17, 163.27, 163.05, 159.61, 158.12, 138.55, 131.54, 131.32, 130.43, 128.92, 128.47, 124.40, 127.15, 121.27, 115.16, 114.76, 111.67, 78.84, 75.99, 55.95, 55.88 ppm; HRMS: *m/z*: calcd for $C_{26}H_{20}N_2O_2$: 393.1603 $[M+H]^+$; found: 393.1583.

4-(3-Chlorophenyl)-6-[4-(prop-2-yn-1-yloxy)phenyl]pyrimidin-2-amine (MVB-15): Orange solid. Yield: 66%; m.p. 126–128 °C; ^{1}H NMR ($CDCl_3$, 400 MHz): $\delta=8.04$–8.02 (m, 3H), 7.90–7.88 (m, 1H), 7.44–7.38 (m, 2H), 7.35 (s, 1H), 7.07–7.04 (m, 2H), 5.25 (s, 2H), 4.74 (s, 2H), 2.54 ppm (s, 1H); ^{13}C NMR ($CDCl_3$, 100 MHz): $\delta=165.89$, 164.58, 163.61, 159.67, 139.74, 134.95, 130.79, 130.41, 128.73, 127.35, 125.24 115.13, 103.57, 78.81, 76.03, 55.93 ppm; HRMS: *m/z*: calcd for $C_{19}H_{14}ClN_3O$: 336.0904 $[M+H]^+$; found: 336.0865.

4-(4-Chlorophenyl)-2-phenyl-6-[2-(prop-2-yn-1-yloxy)phenyl]pyrimidine (MVB-16): Cream solid. Yield: 74%; m.p. 124–126 °C; ^{1}H NMR ($CDCl_3$, 400 MHz): $\delta=8.67$–8.65 (m, 2H), 8.32 (s, 1H), 8.28–8.19 (m, 3H), 7.52–7.39 (m, 6H), 7.24–7.20 (m, 1H), 7.13 (d, $J_{12}=$ 8 Hz, 1H), 4.81 (s, 2H), 2.57 ppm (s, 1H); ^{13}C NMR ($CDCl_3$, 100 MHz): $\delta=164.35$, 163.22, 162.59, 156.23, 138.25, 136.79, 136.33, 131.62, 130.65, 129.12, 128.77, 128.54, 127.42, 127.49, 122.37, 115.30, 113.30, 78.37, 76.10, 56.73 ppm; HRMS: *m/z*: calcd for $C_{25}H_{17}ClN_2O$: 397.1108 $[M+H]^+$; found: 397.1100.

4-(4-Chlorophenyl)-2-phenyl-6-[4-(prop-2-yn-1-yloxy)phenyl]pyrimidine (MVB-17): White solid. Yield: 72%; m.p. 136–138 °C; ^{1}H NMR ($CDCl_3$, 400 MHz): $\delta=8.68$–8.65 (m, 2H), 8.26–8.18 (m, 4H), 7.87 (s, 1H), 7.52–7.49 (m, 5H), 7.13–7.11 (m, 2H), 4.76 (s, 2H), 2.56 ppm (s, 1H); ^{13}C NMR ($CDCl_3$, 100 MHz): $\delta=164.49$, 164.30, 163.34, 159.90, 138.10, 136.95, 136.09, 130.79, 129.19, 128.88, 128.60, 128.55, 115.24, 109.25, 78.19, 76.08, 55.95 ppm; HRMS: *m/z*: calcd for $C_{25}H_{17}ClN_2O$: 397.1108 $[M+H]^+$; found: 397.1095.

2-Phenyl-4-[4-(prop-2-yn-1-yloxy)phenyl]-6-(*p*-tolyl)pyrimidine (MVB-18): White solid. Yield: 64%; m.p. 130–132 °C; ^{1}H NMR ($CDCl_3$, 400 MHz): $\delta=8.71$–8.69 (m, 2H), 8.27–8.25 (m, 2H), 8.18–8.16 (m, 2H), 7.90 (s, 1H), 7.53–7.50 (m, 3H), 7.34 (d, $J=8$ Hz, 2H), 7.13–7.20 (m, 2H) 4.76 (s, 2H), 2.56 ppm (s, 1H); ^{13}C NMR ($CDCl_3$, 100 MHz): $\delta=164.53$, 164.35, 163.96, 159.75, 141.14, 138.40, 138.40, 134.87, 131.00, 130.60, 129.70, 128.84, 128.50, 127.23, 115.20, 109.24, 78.25, 76.03, 55.95 ppm; HRMS: *m/z*: calcd for $C_{26}H_{20}N_2O$: 377.1654 $[M+H]^+$; found: 377.1624.

4-(3-Chlorophenyl)-2-phenyl-6-[4-(prop-2-yn-1-yloxy)phenyl]pyrimidine (MVB-19): White solid. Yield: 78%; m.p. 116–118 °C; ^{1}H NMR ($CDCl_3$, 400 MHz): $\delta=8.69$–8.66 (m, 2H), 8.27–8.24 (m, 3H), 8.12–8.09 (m, 1H), 7.87 (s, 1H), 7.53–7.46 (m, 5H), 7.14–7.10 (m, 2H), 4.77 (s, 2H), 2.57 ppm (s, 1H); ^{13}C NMR ($CDCl_3$, 100 MHz): $\delta=$ 164.53, 164.37, 163.14, 159.95, 139.47, 136.54, 136.12, 130.84, 130.72, 128.90, 128.57, 128.53, 127.45, 125.39, 115.25, 114.71, 109.54, 78.21, 76.09, 55.95 ppm; HRMS: *m/z*: calcd for $C_{25}H_{17}ClN_2O$: 397.1108 $[M+H]^+$; found: 397.1100.

4-(4-Methoxyphenyl)-2-phenyl-6-[4-(prop-2-yn-1-yloxy)phenyl]-pyrimidine (MVB-20): White solid. Yield: 82%; m.p. 119–121 °C; ^{1}H NMR ($CDCl_3$, 400 MHz): $\delta=8.70$–8.68 (m, 2H), 8.26–8.23 (m, 4H), 7.85 (s, 1H), 7.54–7.49 (m, 3H), 7.13–7.10 (m, 2H), 7.05–7.02 (m, 2H), 4.76 (s, 2H), 3.88 (s, 3H), 2.56 ppm (s, 1H); ^{13}C NMR ($CDCl_3$, 100 MHz): $\delta=164.06$, 163.84, 161.92, 159.71, 138.44, 131.06, 130.56, 130.11, 128.82, 128.48, 115.18, 114.29, 108.71, 78.27, 76.03, 55.95, 55.53 ppm; HRMS: *m/z*: calcd for $C_{26}H_{20}N_2O_2$: 393.1603 $[M+H]^+$; found: 393.1586.

Biological studies

Determination of hMAO inhibition: A fluorimetric method was used to evaluate the activity of test compounds against MAO-A and MAO-B enzyme isoforms using an Amplex Red assay kit.[17] In brief, sodium phosphate buffer (0.05 M, pH 7.4, 100 μL) containing the test compounds and reference inhibitors in various concentrations along with sufficient amounts of recombinant hMAO enzyme (hMAO-A: 1.1 μg protein; specific activity: 150 nmol of *p*-tyramine oxidized to *p*-hydroxyphenylacetaldehyde per min per mg protein; hMAO-B: 7.5 μg protein; specific activity: 22 nmol of *p*-tyramine oxidized to *p*-hydroxyphenylacetaldehyde per min per mg protein) were incubated for 15 min at 37 °C in a flat-bottom 96-well plate (Tarsons). After this incubation period, the reaction was started by adding (final concentrations) Amplex Red reagent (200 μM), horseradish peroxidase (1 U mL^{-1}) and *p*-tyramine (1 mM). After 30 min incubation in the dark, the production of H_2O_2 was quantified at 37 °C in a multi-detection microplate fluorescence reader (Synergy H1, BioTek Instruments) based on the fluorescence generated at an emission wavelength of 590 nm upon excitation at 545 nm. Control experiments were carried out simultaneously by replacing the test compounds with vehicle. No fluorescence was observed in the absence of MAO enzyme, thus eliminating the possibility of false readings. The specific final fluorescence emission was calculated after subtraction of the background determined from vials containing all components except the hMAO enzyme, which was replaced by a sodium phosphate buffer solution.

Reversibility studies: Reversibility was studied according to a reported protocol.[18] The test compounds were incubated with the MAO enzymes at $10\times IC_{50}$ and $100\times IC_{50}$ concentrations for 30 min at 37 °C, and 4% DMSO was added as a co-solvent to all samples; a negative control without inhibitor was also prepared. After a 30 min incubation period, the samples were diluted 100-fold with the addition of tyramine substrate to achieve final inhibitor con-

centrations of $0.1\times IC_{50}$ and $1\times IC_{50}$. As positive controls, MAO-A and MAO-B were incubated with the irreversible inhibitors, clorgyline and pargyline, respectively, at $10\times IC_{50}$ concentrations and then diluted 100-fold to achieve final inhibitor concentrations of $0.1\times IC_{50}$. After dilution, the residual MAO activities were measured ($n=3$) and are expressed as mean ± SD.

ROS inhibition studies: Intracellular levels of ROS were determined according to a protocol described elsewhere,[26] using the nonfluorescent compound 2′,7′-dichlorodihydrofluorescein diacetate (H_2DCF-DA). It is permeable through the cell membrane and once internalized it is hydrolyzed by intracellular esterases and oxidized by ROS to the fluorescent 2′,7′-dichlorofluorescein. Cells (SH-SY5Y) were seeded in 96-well plates (1×10^4 cells per well) and left for 24 h in complete media at 37 °C. Then the media was removed, and the cells were washed with phosphate-buffered saline (PBS) and treated with test compounds (without fetal bovine serum) for 24 and 48 h at different concentrations (1 and 10 μM). Thereafter, the media was removed, and the cells were washed with PBS and treated with H_2DCF-DA (50 μM) and incubated for 30 min at 37 °C. Following incubation, cells were rinsed with PBS and fluorescence was measured with excitation and emission wavelengths of 478 and 518 nm, respectively.

Cytotoxicity studies: To test the cytotoxicity of the synthesized compounds on neuronal cells, MTT assays were performed with the human neuroblastoma SH-SY5Y cells. Approximately 10000 cells were seeded per well in a 96-well plate in DMEM/F-12 media containing 10% fetal bovine serum and horse serum supplemented with 1% penicillin and grown for 24 h and treated as indicated.[27] Cells were treated with test compounds (25 μM) for 24 or 48 h in a humidified CO_2 incubator maintained at 37 °C with 5% CO_2 and 95% humidity under serum-free conditions.

Molecular docking studies

To determine the mode of interaction between the synthesized ligands and the active sites of the hMAO-A and hMAO-B enzymes, molecular docking studies were performed using Maestro 11.1 (Schrödinger LLC). An X-ray crystal structure of hMAO-B (PDB ID: 2BYB)[21] enzyme was imported from the RCSB Protein Data Bank (http://www.rscb.org). Protein was prepared using the "protein preparation wizard" application of the Schrödinger suite 2017. Energy was minimized using the OPLS2005 force field. Ligands were drawn in ChemBioDraw Ultra 12 and prepared using the ligand preparation application in Schrödinger suite 2017. For each compound, the top-score docking poses were chosen for final ligand–target interaction analysis using the XP interaction visualizer of Maestro 11.1. Validation of the docking procedure was checked by re-docking a co-crystalized ligand into the active site of the MAO enzyme.

Acknowledgements

V.K. is grateful to the Central University of Punjab (CUP), Bathinda, India, for providing financial assistance in the form of Research Seed Money (RSM G-25). B.K. is grateful to CUP, Bathinda and UGC for a PhD fellowship.

Conflict of interest

The authors declare no conflict of interest.

Keywords: monoamine oxidase · Parkinson's disease · pyrimidines · reversible MAO inhibitors

[1] a) J. Jankovic, *J. Neurol. Neurosurg. Psychiatry* **2008**, *79*, 368–376; b) A. Gaspar, J. Reis, A. Fonseca, N. Milhazes, D. Viña, E. Uriarte, F. Borges, *Bioorg. Med. Chem. Lett.* **2011**, *21*, 707–709.
[2] a) B. Kumar, V. P. Gupta, V. Kumar, *Curr. Drug Targets* **2017**, *18*, 87–97; b) J. K. Mallajosyula, D. Kaur, S. J. Chinta, S. Rajagopalan, A. Rane, D. G. Nicholls, D. A. Di Monte, H. Macarthur, J. K. Andersen, *PLoS One* **2008**, *3*, e1616.
[3] P. Jenner, C. W. Olanow, *Neurology* **1996**, *47*, 161S–170S.
[4] B. S. Connolly, A. E. Lang, *JAMA J. Am. Med. Assoc.* **2014**, *311*, 1670–1683.
[5] C. L. Tomlinson, R. Stowe, S. Patel, C. Rick, R. Gray, C. E. Clarke, *Mov. Disord.* **2010**, *25*, 2649–2653.
[6] P. Riederer, G. Laux, *Exper. Neurobiol.* **2011**, *20*, 1–17.
[7] a) M. Naoi, W. Maruyama, *Expert Rev. Neurother.* **2009**, *9*, 1233–1250; b) O. Bar-Am, T. Amit, M. B. H. Youdim, *J. Neurochem.* **2007**, *103*, 500–508.
[8] B. Kumar, A. K. Mantha, V. Kumar, *RSC Adv.* **2016**, *6*, 42660–42683.
[9] S. Kumar, A. Deep, B. Narasimhan, *Cent. Nerv. Syst. Agents Med. Chem.* **2015**, *15*, 5–10 .
[10] T. P. Selvam, C. R. James, P. V. Dniandev, S. K. Valzita, *Res. Pharm.* **2012**, *2*, 01–09.
[11] B. Mathew, J. Suresh, S. Anbazhagan, *J. Saudi Chem. Soc.* **2016**, *20*, S132–S139.
[12] C. Altomare, S. Cellamare, L. Summo, M. Catto, A. Carotti, U. Thull, P.-A. Carrupt, B. Testa, H. Stoeckli-Evans, *J. Med. Chem.* **1998**, *41*, 3812–3820.
[13] A. Carotti, M. Catto, F. Leonetti, F. Campagna, R. Soto-Otero, E. Méndez-Álvarez, U. Thull, B. Testa, C. Altomare, *J. Med. Chem.* **2007**, *50*, 5364–5371.
[14] J. J. Chen, D. M. Swope, K. Dashtipour, *Clin. Ther.* **2007**, *29*, 1825–1849.
[15] O. Weinreb, S. Mandel, O. Bar-Am, M. Yogev-Falach, Y. Avramovich-Tirosh, T. Amit, M. B. Youdim, *Neurotherapeutics* **2009**, *6*, 163–174.
[16] A. Nimkar, M. M. V. Ramana, R. Betkar, P. Ranade, B. Mundhe, *New J. Chem.* **2016**, *40*, 2541–2546.
[17] F. Chimenti, S. Carradori, D. Secci, A. Bolasco, B. Bizzarri, P. Chimenti, A. Granese, M. Yanez, F. Orallo, *Eur. J. Med. Chem.* **2010**, *45*, 800–804.
[18] a) S. Mostert, W. Mentz, A. Petzer, J. J. Bergh, J. P. Petzer, *Bioorg. Med. Chem.* **2012**, *20*, 7040–7050; b) C. Minders, J. P. Petzer, A. Petzer, A. C. Lourens, *Bioorg. Med. Chem. Lett.* **2015**, *25*, 5270–5276; c) R. Breinbauer, *Angew. Chem. Int. Ed.* **2005**, *44*, 6445; *Angew. Chem.* **2005**, *117*, 6603; d) A. Stößel, M. Schlenk, S. Hinz, P. Küppers, J. Heer, M. Gütschow, C. E. Müller, *J. Med. Chem.* **2013**, *56*, 4580–4596.
[19] M. D. Mertens, S. Hinz, C. E. Müller, M. Gütschow, *Bioorg. Med. Chem.* **2014**, *22*, 1916–1928.
[20] a) N. Pizzinat, N. Copin, C. Vindis, A. Parini, C. Cambon, *Naunyn-Schmiedeberg's Arch. Pharmacol.* **1999**, *359*, 428–431; b) A. Sturza, L. Noveanu, O. Duicu, D. Angoulvant, D. M. Muntean, *Arch. Cardiovascul. Disease Suppl.* **2014**, *6*, 15.
[21] L. De Colibus, M. Li, C. Binda, A. Lustig, D. E. Edmondson, A. Mattevi, *Proc. Natl. Acad. Sci. USA* **2005**, *102*, 12684–12689.
[22] E. M. Milczek, C. Binda, S. Rovida, A. Mattevi, D. E. Edmondson, *FEBS J.* **2011**, *278*, 4860–4869.
[23] S.-Y. Son, J. Ma, Y. Kondou, M. Yoshimura, E. Yamashita, T. Tsukihara, *Proc. Natl. Acad. Sci. USA* **2008**, *105*, 5739–5744.
[24] D. E. Edmondson, C. Binda, A. Mattevi, *Arch. Biochem. Biophys.* **2007**, *464*, 269–276.
[25] V. Kumar, B. Kumar, A. R. Dwivedi (Central University of Punjab, Bathinda, India), Indian Patent No.201811008301, **2018**.
[26] N. Kaur, M. Dhiman, J. R. Perez-Polo, A. K. Mantha, *J. Neurosci. Res.* **2015**, *93*, 938–947.
[27] B. Kumar, Sheetal, A. K. Mantha, V. Kumar, *Bioorg. Chem.* **2018**, https://doi.org/10.1016/j.bioorg.2018.01.020.

Manuscript received: September 23, 2017
Revised manuscript received: November 4, 2017
Version of record online: March 13, 2018